Enhancement of antioxidative activity of astaxanthin by combination with an antioxidant capable of forming intermolecular interactions

Tatsuya Fukuta,[1,#] Shota Hirai,[1,#] Tatsusada Yoshida,[2] Takashi Maoka,[3] Kentaro Kogure[1,*]

[1]*Department of Pharmaceutical Health Chemistry, Graduate School of Biomedical Sciences, Tokushima University, Shomachi 1, Tokushima 770-8505, Japan*

[2]*Faculty of Pharmaceutical Sciences, Nagasaki International University, Nagasaki, 859-3298, Japan*

[3]*Research Institute for Production Development, Shimogamo, Morimoto-Cho, Sakyo-ku, Kyoto, 606-0805, Japan*

[*]Correspondence author: Kentaro Kogure

TEL: +81-88-633-7248

FAX: +81-88-633-9572

Email: kogure@tokushima-u.ac.jp

Department of Pharmaceutical Health Chemistry, Graduate School of Biomedical Sciences, Tokushima University, Shomachi 1, Tokushima 770-8505, Japan

[#]These authors contributed equally to this work

Running title: Capsaicin enhances astaxanthin action in liposomes

Abstract

We previously demonstrated that co-encapsulation of the potent antioxidant astaxanthin (Asx) and tocotrienols into liposomes results in synergistically higher antioxidative activity than the calculated additive activity of each individual antioxidant-containing liposome, due to intermolecular interactions between terminal ring moieties of the two antioxidants and the polyene chain and the triene moiety. We reported that intermolecular interactions depend on the stereochemistry of Asx, and change the electronic state of the Asx polyene moiety. Based on these findings, we hypothesized that antioxidants that interact with Asx at the terminal ring and polyene moieties may enhance the antioxidative activity. Herein, we selected two candidate antioxidants, capsaicin (Cap) and resveratrol, based on their structures, in which the compounds exhibit similar characteristics to tocotrienols. We evaluated the antioxidative capacities of liposomes co-encapsulating Asx and the selected candidates. Based on hydroxyl radical scavenging activity, Cap was found to synergistically enhance the antioxidative activity of Asx at an optimal Asx/Cap ratio. Intermolecular interactions between Asx and Cap are necessary for the synergistic effect, and the Asx stereoisomer 3*R*,3'*R*-form (Asx-*R*) was predicted to most potently interact. Liposomes co-encapsulating Asx-*R* and Cap exhibited clear synergistic antioxidative activity at an optimal ratio, whereas liposomes co-encapsulating the other Asx stereoisomer and Cap did not demonstrate such activity. Computational chemistry analysis showed that changes in the electronic state of the polyene moiety of Asx-*R* are crucial for the synergistic activity. These results suggest that antioxidants that can change the electronic state of Asx via intermolecular interactions may enhance the function of Asx.

Keywords

Antioxidants; Astaxanthin; Liposomes; Capsaicin; Intermolecular interactions; Stereochemistry

Introduction

As oxidative stress induced by excess reactive oxygen species (ROS) is involved in the progression of various diseases, such as arteriosclerosis, dry eye, and ischemic stroke [1-3], suppression of oxidative stress by certain therapeutic agents is a feasible therapeutic strategy for the treatment of such diseases. In fact, the radical scavenger edaravone has been approved in a limited number of countries for the treatment of acute ischemic stroke via suppression of ROS-mediated brain damage after cerebral ischemia/reperfusion [4]. Hence, it is expected that antioxidants that possess potent ROS-scavenging capabilities could represent potential agents for the prevention and treatment of ROS-related diseases.

The carotenoid astaxanthin (Asx, 3,3'-dihydroxy-β,β-carotene-4,4'-dione) has been reported to be a more potent antioxidant than the representative compounds carotenoid β-carotene and vitamin E α-tocopherol for the prevention of singlet oxygen and suppression of lipid peroxidation in biological membranes [5-7]. Also, upon incorporation of highly hydrophobic Asx into liposome membranes to evaluate antioxidative activity in aqueous conditions, we previously found that Asx can effectively scavenge hydroxyl radicals [8]. Moreover, our previous study demonstrated that transdermal delivery of liposomes encapsulating Asx (Asx-lipo) via iontophoresis can prevent ultraviolet-induced melanin production in the skin due to the potent radical-scavenging ability of Asx [9]. Based on these findings, application of Asx may prevent pathological progression of ROS-related diseases. In addition, as Asx is broadly used as a cosmetic ingredient and a nutritional supplement, its application in humans has been demonstrated to be safe.

To increase the antioxidative ability of Asx-lipo, we demonstrated that co-encapsulation of Asx and one type of vitamin E, namely α-tocotrienol (α-T3), into liposomes results in synergistically higher antioxidative activity *in vitro* than the calculated additive activity of each of the individual antioxidant-containing liposomes [10]. The synergistic effect was shown to result from intermolecular interactions via hydrogen bonding between the terminal ring of Asx and the chroman ring of α-T3 and via partial interaction of the polyene chain of Asx and the triene chain of α-T3 [10].

We recently reported additional details of the synergistic mechanism, noting that the stereochemistry of Asx is an important factor for the higher antioxidative activity of liposomes co-encapsulating Asx and α-T3 compared with the additive activity of liposomes encapsulating the individual single agents [11]. Moreover, changes in the electronic structures of the polyene moiety upon interaction of Asx with α-T3 were suggested to be crucial for the enhancement of their antioxidative activity based on results of a computational chemistry analysis. Based on these findings, we hypothesized that other antioxidants that can interact with Asx at the terminal ring moiety and the polyene moiety in liposomal membranes may enhance the antioxidative activity of Asx. Moreover, liposomes co-encapsulating Asx and the candidate compounds may offer new and promising antioxidant formulations.

In the present study, we selected two candidate antioxidants, capsaicin (Cap) and resveratrol (Res), based on their structures, in which the compounds exhibit both phenolic OH and hydrophobic side chain group similar to α-T3 (Fig. 1). Cap is an alkaloid found in chili pepper and has an analgesic effect as well as antioxidative effects [12,13]. Res is a polyphenol that is known to exhibit antioxidative and anti-inflammatory effects, and is found in foods such as red wine and grape peels [14,15]. By preparing liposomes encapsulating each candidate antioxidant, we first evaluated their antioxidative capacities based on their ability to scavenge hydroxyl radicals. We then evaluated the antioxidative effects of liposomes co-encapsulating Asx and the candidate antioxidants *in vitro*. Computational chemistry analysis was carried out to evaluate intermolecular interactions induced in liposomes co-encapsulating multiple antioxidants.

Materials and methods

Materials

Synthetic Asx was purchased from Sigma-Aldrich (St. Louis, USA). 3*S*,3'*S*- (Asx-*S*) was gifted from Fuji Chemical Industries (Toyama, Japan). Capsaicin (Cap) was obtained from Wako Pure Chemical (Osaka, Japan), and resveratrol (Res) from Tokyo Chemical Industry (Tokyo, Japan). Egg phosphatidylcholine (EPC) was purchased from NOF Corporation (Tokyo, Japan). Aminophenyl fluorescein (APF) was obtained from Goryo Chemical (Sapporo, Japan). All other reagents used in this study were of the highest grade available commercially.

Preparation of liposomes encapsulating Asx and other antioxidants

Liposomes composed of EPC, Asx, and other antioxidants were prepared by the thin-film method. Chloroform solution containing 2 μmol of EPC, and each of the tested concentrations of Asx and the other antioxidants, was added to test tubes and dried using nitrogen gas. The dried lipid film was hydrated with 0.2 mL of 10 mM Tris-HCl buffer (pH 7.4) at room temperature, and liposomes were prepared by sonication using a bath-type sonicator. The particle sizes of the resultant liposomes were measured with a Zetasizer Nano ZS (Malvern Instruments, Worcestershire, UK). The diameters of the liposomes used in this study were determined to be 150–250 nm.

Evaluation of hydroxyl radical scavenging activity of liposomes

The production of hydroxyl radicals was evaluated by measuring the fluorescence intensity of APF [16]. To generate hydroxyl radicals, 30 μL of 10 mM H_2O_2 (final conc.: 1 mM), 45 μL of each liposomal suspension at a concentration of 10 mM (final lipid conc.: 1.5 mM), 30 μL of 100 μM APF solution (final conc.: 10 μM), and 30 μL of 1 mM $FeSO_4$ solution (final conc.: 100 μM) were mixed in a test tube. Using this protocol, hydroxyl radicals are generated via the Fenton reaction as follows: $Fe^{2+} + H_2O_2 \rightarrow Fe^{3+} + OH^- + \cdot OH$ [17]. After mixing, the fluorescence intensity

(excitation: 490 nm; emission: 515 nm) was measured within 10 seconds with a Tecan Infinite M200 microplate reader (Salzburg, Switzerland). The decrease rate of the fluorescence intensity of APF in each group was calculated as the hydroxyl radical scavenging activity by setting the control group as 100%. In the control group, 45 µl of 10 mM plane EPC liposomes (final lipid conc.: 1.5 mM) was added to the sample tube instead of each antioxidant-containing liposomes. In case of evaluating additive antioxidative activity, the final lipid concentration in a test tube was 3.0 mM by adding 45 µL of two species of antioxidant-containing liposomes, respectively. For evaluating synergistic activity, the final lipid concentration in a test tube was also 3.0 mM by adding 45 µL of antioxidants co-encapsulating and 45 µL of plain EPC liposomes.

Estimation of the intermolecular interaction energy between each Asx stereoisomer and Cap

All calculations were performed using the Gaussian 09 program. The B3LYP-D3(BJ) hybrid density functional theory (DFT) was employed, which contains Grimme's empirical dispersion correction (D3(BJ)) term [18]. The minimum energy conformations of the Asx stereoisomers, Asx-*S*, Asx-*R*, and 3*R*,3'*S*-form (Asx-*meso*), with Cap were first calculated with calculated mechanics. Based on the calculated conformations, optimized structures were then predicted using semi-empirical molecular calculations. Intermolecular interaction energies were estimated using the difference in heats of formation for each of the following combinations: Asx-*S*-Cap, Asx-*R*-Cap, and Asx-*meso*-Cap.

Visible absorption spectra of antioxidant-containing liposomes

The visible absorption spectra between 400 and 600 nm of liposomes encapsulating Asx-*R* (Asx-*R*-lipo), liposomes encapsulating Cap (Cap-lipo), and liposomes co-encapsulating Asx-*R* and Cap (Asx-*R*/Cap-lipo) at a 2:1 molar ratio of Asx-*R*/Cap were measured with a NanoPhotometer C40 (Implen GmbH, Munich, Germany). The concentrations of each liposome were the same as described above. The absorption spectrum of plain EPC liposomes was subtracted from that of

liposomes encapsulating each antioxidant to cancel out the turbidity of the liposomes.

Prediction of the influence of intermolecular interactions with Cap on the electronic state of Asx-R

Electronic calculations were carried out using the Gaussian 09 program. The initial structure of the Asx-*R*/Cap complex was prepared based on according to previously reported methods [10,19]. The geometries of the complex and Asx-*R* alone were then completely optimized by the 6-31G(d) basis set. The zero-point energy (ZPE) corrected hemolytic C-H bond dissociation energy (BDE) was calculated at the B3LYP-D3(BJ)/6-311+G(d,p)//B3LYP-D3(BJ)/6-31G(d) level for Asx-*R*, both in the Asx-*R*/Cap complex and alone. To investigate changes in charge distribution within Asx-*R* owing to complex formation with Cap, $\Delta qi(\text{Asx-}R)(=qi(\text{Asx-}R)_{complex}-qi(\text{Asx-}R)_{alone})$, natural population analysis [20] was performed at the same level. $qi(\text{Asx-}R)_{complex}$ and $qi(\text{Asx-}R)_{alone}$ denote the natural charges on the i-th atom within Asx-*R* in the complex and alone, respectively. The contribution of hydrogen atoms to $\Delta qi(\text{Asx-}R)$ was summed into the heavy atoms.

Statistical analysis

Statistical differences between groups were evaluated using the Student's *t-test*. Data are presented as mean ± standard deviation (S.D.).

Results

Evaluation of antioxidative activity of liposomes encapsulating Cap or Res

Because Cap and Res contain both phenolic OH and hydrophobic side chain groups (Fig. 1), both of which were shown to be important for intermolecular interaction of α-T3 with Asx in our previous studies [10,11], we selected Cap and Res as candidate antioxidants to enhance the antioxidative activity of Asx by co-encapsulation into liposomes. First, we evaluated the antioxidative activities of liposomes encapsulating Cap (Cap-lipo) and Res (Res-lipo) based on their abilities to scavenge hydroxyl radicals. The particle diameters of the liposomes used in the following experiments were adjusted to 150-250 nm. We used the reagent APF, which fluoresces upon reaction with hydroxyl radicals. Results demonstrated that both Cap-lipo and Res-lipo showed dose-dependent hydroxyl radical-scavenging abilities (Fig. 2). Moreover, upon comparison of the effect of Cap-lipo and Res-lipo at identical concentrations, the hydroxyl radical-scavenging effect of Cap-lipo was found to be higher than that of Res-lipo.

Antioxidative effect of liposomes co-encapsulating Asx and each candidate antioxidant

Next, we evaluated the hydroxyl radical scavenging activities of liposomes co-encapsulating Asx and Cap (Asx/Cap-lipo) or Res (Asx/Res-lipo). The activities were augmented with increasing amounts of Asx (Figs. 3A and B). By fixing the concentrations of Cap and Res at 0.94 and 1.88 μM, respectively, we sought to identify the optimal ratios of Asx/Cap and Asx/Res that results in the highest antioxidative activities compared with the additive effects of each of the individual antioxidant-containing liposomes. As shown in Fig. 3A, the activity of Asx/Res-lipo was nearly the same as or lower than the calculated additive activities of Asx-lipo and Res-lipo, implying that this combination did not exhibit synergistic antioxidative activity. On the other hand, the hydroxyl radical scavenging activity of Asx/Cap-lipo was higher than the sum of the activities of Asx-lipo and Cap-lipo at an Asx/Cap ratio of 2:1, whereas the activities of Asx/Cap-lipo at other ratios were

comparable to the sum of the liposomes containing each of the individual agents (Fig. 3B). By mixing Asx-lipo and Cap-lipo at an Asx/Cap ratio of 2:1, or adding Asx/Cap-lipo (Asx:Cap=2:1) in test tubes, we evaluated additive and synergistic hydroxyl radical scavenging activities. As shown in Fig. 3C, Asx/Cap-lipo (Asx:Cap=2:1) showed a 1.66-fold synergistically higher hydroxyl radical scavenging activity compared with the additive activity of liposomes containing individual agents. These results suggest that an Asx/Cap ratio of 2:1 is optimal to exert efficient antioxidative activities in liposomal membranes.

Comparison of intermolecular interaction energies between stereoisomers of Asx and Cap

As a synergistic antioxidative activity was observed upon co-encapsulation of Asx and Cap into liposomes at a ratio of 2:1, we hypothesized that intermolecular interactions may be formed between Asx and Cap within the liposomal membranes, similar to those observed for liposomes co-encapsulating Asx/α-T3 in our previous study [11]. Further, Asx exhibits three known stereoisomers, namely 3*S*,3'*S*-form (Asx-*S*), 3*R*,3'*R*-form (Asx-*R*), and 3*R*,3'*S*-*meso* form (Asx-*meso*) [21] (Fig. 1). The synthetic Asx used in our above-mentioned experiments consisted of a mixture of these three stereoisomers at a ratio of Asx-*S*/Asx-*R*/Asx-*meso*=1:1:2 [21]. We compared the intermolecular interaction energies between the stereoisomers of Asx and Cap by computational chemistry analysis. By employing the B3LYP method, the heats of intermolecular interaction of Asx-*S*, Asx-*R*, and Asx-*meso* with Cap were determined to be 26.05, 29.04, and 27.62 kcal/mol, respectively (Fig. 4). These results suggest that Asx-*R* forms more energetically stable intermolecular interactions with Cap compared to Asx-*S* and Asx-*meso*.

Antioxidative activity of liposomes co-encapsulating different stereoisomers of Asx and Cap

Based on the differences in the heats of intermolecular interaction between Asx stereoisomers, we compared the hydroxyl radical scavenging activities of liposomes co-encapsulating Asx-*S*/Cap (Asx-*S*/Cap-lipo) and Asx-*R*/Cap (Asx-*R*/Cap-lipo). The activity of

Asx-*S*/Cap-lipo was lower than the calculated additive activity of Asx-*S*-lipo and Cap-lipo (Fig. 5A). On the other hand, the activity of Asx-*R*/Cap-lipo, of which particle size was adjusted to 150-170 nm by extrusion through polycarbonate membrane filter with 200-nm pores, was higher than the additive activities of Asx-*R*-lipo and Cap-lipo at Asx/Cap ratios of 1:2 or 1:1, whereas the activities of Asx-*R*/Cap-lipo at other ratios were nearly the same as the sum of those of liposomes encapsulating the individual agents (Fig. 5B). By mixing Asx-R-lipo and Cap-lipo at an Asx-R/Cap ratio of 1:2, or adding Asx-R/Cap-lipo (Asx-R:Cap=1:2) in test tubes, the additive and synergistic hydroxyl radical scavenging activities were evaluated. As shown in Fig. 5C, Asx-R/Cap-lipo (Asx-R:Cap=1:2) showed significantly higher (1.48-fold) synergistic hydroxyl radical scavenging activity compared with the additive activity of liposomes containing individual agents. These results suggest that the stronger intermolecular interactions between Asx-*R* and Cap compared with Asx-*S* and Cap contributed to the synergistically higher hydroxyl radical scavenging activity at the optimal ratio (Asx-*R*/Cap=1:2).

Changes in electronic state of Asx-R via intermolecular interaction with Cap

Our previous study reported that the hydrogen atoms at C3/C3' in the Asx terminal ring moieties act as active sites for scavenging ROS via extraction of a free radical [6] (Fig. 6). The active site of Cap for scavenging ROS was also previously reported to be the hydrogen atom at C7, as shown by the dotted circle in Fig. 6 [12]. We hypothesized that the reactivity of the active sites of Asx-*R* and Cap may be changed via formation of intermolecular interactions. We estimated the activity of Asx-*R* and Cap by calculating the bond dissociation energy (BDE) between C3 and H for Asx, and between C7 and H for Cap. Results showed that the H-C3 BDE in Asx-*R* alone and Asx-*R*-Cap were 68.82 kcal/mol and 68.56 kcal/mol, respectively. On the other hand, the H-C7 BDE in Cap alone and in the Asx-*R*-Cap complex were 78.36 kcal/mol and 78.33 kcal/mol, respectively (Fig. 6). These results imply that, unexpectedly, the reactivity of the active sites of Asx and Cap was nearly unchanged via intermolecular interactions.

Asx is known to be able to scavenge free radicals via both the polyene chain as well as the terminal ring moieties [6]. Our previous study demonstrated that intermolecular interaction of Asx with α-T3 causes changes in the electronic state of the Asx polyene moiety by the presence of the double bond in the α-T3 triene moiety [11]. Based on these findings, we hypothesized that a change in the electronic state of the Asx-*R* polyene moiety is induced via intermolecular interaction with Cap within the liposomal membranes. To confirm the change in the electronic state of Asx-*R*, the visible absorption spectrum of Asx-*R*/Cap-lipo prepared at the optimal ratio of 1:2 was compared with the combined visible absorption spectra of Asx-*R*-lipo and Cap-lipo. The spectrum of Asx-*R*/Cap-lipo, which is dominated by Asx-*R*, was different from the combined spectrum of Asx-*R*-lipo and Cap-lipo, with the peak of the visible absorption being slightly shifted upon co-encapsulation (Fig. 7). These results suggest that the electronic state of Asx-*R* was influenced by intermolecular interactions with Cap.

Next, the effect of intermolecular interaction with Cap on the electronic structure of Asx-*R* was investigated by computational chemistry. The electronic structures of Asx-*R* half fragment A, which interacted with Cap, were compared with that of free Asx-*R* fragment B (Fig. 8A). Intermolecular interactions with Cap resulted in marked changes in the electronic charges on the C7, C8, C9, C12, and C14 atoms in Asx-*R* (Fig. 8B), while the electronic structures of Cap was nearly unchanged (Fig. 8C). Surprisingly, the electronic charges on the C3 and H atoms in Asx-*R* half fragment, which are active sites for scavenging ROS, were unchanged, in contrast to those in Asx-*R* half fragment B. These results suggest that changes in the electronic structures of the polyene moiety of Asx-*R* upon intermolecular interaction may be responsible for the increased synergistic antioxidative activity of Asx-*R*/Cap-lipo.

Discussion

Asx has been reported to be a superior antioxidant compared with representative antioxidants such as β-carotene and α-tocopherol, owing to its high activity for prevention of ROS production and lipid peroxidation in biological membranes [5-7]. Hence, Asx is not only used as a nutritional supplement and a cosmetic ingredient, but may also exhibit the potential as a treatment of ROS-related diseases [22-25]. To augment the antioxidative activity of Asx, we previously constructed liposomes co-encapsulating Asx and α-T3, and succeeded in the synergistic enhancement of the antioxidative activity resulting from intermolecular interactions via hydrogen bonding formation between the terminal ring of Asx and the chroman ring of α-T3 in the liposomal membranes [10]. We also demonstrated that changes in the electronic structure of the polyene moiety of Asx upon interaction with the α-T3 triene moiety were crucial for the synergistic increase in Asx antioxidative activity [11]. As the intermolecular interactions in the terminal ring moiety and polyene moiety of Asx were demonstrated to be important for the enhancement of the antioxidative activity of Asx, we hypothesized that other antioxidants that can also form intermolecular interactions with Asx at the terminal ring moiety and the polyene moiety may function as enhancers of the antioxidative activity of Asx.

As candidate antioxidants for exploring enhancers of Asx activity, we selected Cap and Res based on their structures, as they exhibit both phenolic OH and hydrophobic side chain groups, similar to α-T3 (Fig. 1). These hydrophobic antioxidants were incorporated into liposomal membranes to evaluate their antioxidative activities under aqueous conditions. Also, the particle diameters of the liposomes used in the present study were adjusted to 150-250 nm. Thus, the antioxidative activities of each liposomal antioxidant could not be influenced by the size of the liposomes. Both Cap-lipo and Res-lipo showed dose-dependent hydroxyl radical scavenging effects, although the effect of Cap-lipo was higher than that of Res-lipo at the same concentration (Fig. 2). Co-encapsulation of Res with Asx resulted in a hydroxyl radical scavenging activity for Asx/Res-lipo that was nearly the same or lower than the calculated additive activity of Asx-lipo and Res-lipo (Fig.

3A). As to the reason why the combination of Res with Asx did not show enhancement of Asx antioxidative activity, we speculate that the benzene ring in the hydrophobic side chain group of Res impeded formation of intermolecular interaction with Asx within the liposomal membranes. On the other hand, the antioxidative activity of Asx/Cap-lipo (ratio of 2:1) was significantly higher than the additive value of liposomes encapsulating the individual agents (Figs. 3B and C). These results suggest that Cap may enhance the antioxidative activity of Asx, and that the optimal Asx/Cap ratio in the liposomal membranes could be 2:1.

To elucidate the underlying mechanism of the synergistic antioxidative activity of Asx/Cap-lipo at a ratio of 2:1, intermolecular interactions between Asx and Cap were investigated by computational chemistry. The intermolecular interaction energies between Cap and each of the three stereoisomers of Asx (Asx-*S*, Asx-*R*, and Asx-*meso*) were calculated. Interestingly, the heats of intermolecular interaction were different among the three stereoisomers, with that of the Asx-*R*-Cap complex being the highest (Fig. 4), implying that Asx-*R* exhibits the most potent intermolecular interaction with Cap and that a molecular complex of Asx-*R* with Cap in liposomal membranes is favorable over molecular pairs containing either Asx-*S* or Asx-*meso*. Hydroxyl radical scavenging activities of liposomes co-encapsulating either Asx-*S* or Asx-*R* and Cap showed that the activity of Asx-*S*/Cap-lipo was lower than the additive activity of liposomes encapsulating the individual agents at each ratio studied (Fig. 5A). However, Asx-*R*/Cap-lipo at a ratio of 1:2 exhibited remarkable synergistic activity (Figs. 5B and C), suggesting that the optimal ratio of Asx-*R* and Cap in liposomal membranes is likely 1:2, which is different from the optimal ratio found for synthetic Asx and Cap (i.e., 2:1). As the molar ratio of the stereoisomers in synthetic Asx is known to be Asx-*S*/Asx-*R*/Asx-*meso*=1:1:2 [21], the relative molar ratio of Asx-*R* in 1 mol of synthetic Asx is presumed to be 0.25. Based on this estimation, the relative amount of Asx-*R* in liposomes encapsulating synthetic Asx/Cap (2:1) would be 0.5, suggesting that the relative molar ratio of Asx-*R*/Cap in the Asx-*R*/Cap-lipo was 1:2. This estimation is thought to be consistent with the results shown in Fig. 5.

To elucidate the mechanism of the synergistic activity of Asx-*R*/Cap-lipo, the BDEs at the active sites of Asx-*R* and Cap, namely H-C3 of Asx-*R* and H-C7 of Cap, under the complex conditions were individually compared with those of either Asx-*R* or Cap alone. Surprisingly, the BDEs of both Asx-*R* and Cap were mostly unchanged under both the simple and complex conditions, indicating that the reactivity of the active sites of both antioxidants was not affected by intermolecular interactions. On the other hand, results of a computational chemistry analysis found that the electronic state of the polyene moiety of Asx-*R* was markedly changed upon intermolecular interaction with Cap (Fig. 8), whereas the electronic state of Cap was largely unaffected. In particular, electronic charges on the C7, C8, C9, C12, and C14 atoms in Asx-*R* were markedly changed via intermolecular interaction with Cap (Fig. 8B). Additionally, visible absorption spectra also indicated that the electronic state of Asx-*R* was influenced by intermolecular interactions (Fig. 7), similar to the changes found for the electronic state of Asx-*S* upon co-encapsulation with α-T3 in our previous study [11]. Based on these results, changes in the electronic state of the Asx-*R* polyene moiety by intermolecular interaction with Cap may be responsible for the synergistic enhancement of the antioxidative activity of Asx. With regard to the formation of intermolecular interactions between Asx stereoisomers and other antioxidants, the ideal partner for Asx-*R* was Cap, whereas that for Asx-*S* was α-T3. As these differences are thought to result from structural properties of the paired compound for Asx, it is important to take into account the properties of the compounds to be combined with Asx as antioxidative activity enhancers.

As to the distribution of the antioxidant molecules in the liposomal membranes, since liposomes composed of EPC have high membrane fluidity, the antioxidant molecules should freely distribute in the membranes. In addition, our previous study reported that Asx encapsulated in the liposomal membranes can form both intermolecular and intramolecular hydrogen bonding in the membrane [6]. Regarding intermolecular interaction, we reported that the two terminal rings of Asx interact with the hydrophilic polar region of membrane phospholipids. In the case of intramolecular interaction, the hydroxyl and carbonyl groups of Asx form intramolecular hydrogen-bonded

five-membered ring, which increases the hydrophobicity of Asx advantageous for its location inside the membrane. Therefore, the terminal rings of Asx can be located either inside the membrane or at/near the membrane surface. Similarly to Asx, we previously reported that the phenolic hydrogen and acetylic oxygen of Cap possibly form hydrogen bonds with polar groups of membrane phospholipids, resulting in close location of the reaction site C7-benzyl carbon to the membrane surface [12]. Also, Cap forms an intramolecular hydrogen bond, and the hydrogen-bonded intramolecular five membered ring formation should increase the hydrophobicity of the ring moiety, which causes the vanillyl region of Cap to enter into the interior of the membrane. Hence, Cap can also be located either inside the membrane or at/near the surface of the membranes. Considering these findings, the antioxidant molecules can freely move in the liposomal membranes, such as from inner leaflets to outer ones. Consequently, it was suggested that both Asx, especially Asx-R, and Cap existing either inside the membrane or at/near the membrane surfaces could form intermolecular interactions in the each region, and exert synergistic antioxidative activity.

Based on the findings in the present study and our previous studies, it is suggested that antioxidants, such as Cap and α-T3, that can intermolecularly interact with Asx at the terminal ring and polyene moieties could act as enhancers of the antioxidative activity of Asx. Although we have shown the usefulness of liposomes co-encapsulating Asx and other antioxidants (Cap and α-T3) that can enhance the function of Asx *in vitro*, demonstration of the antioxidative capacity of those liposomes *in vivo* is needed for future therapeutic applications involving the treatment of various ROS-related diseases.

In conclusion, we found that the antioxidant Cap can enhance the antioxidative activity of Asx upon co-encapsulation into liposomal membranes. The stereochemistry of Asx was found to be an important factor for effective formation of intermolecular interactions to exert synergistic antioxidative activities of Asx-*R*/Cap-lipo. The optimal ratio of Asx-*R*/Cap in liposomes was determined to be 1:2. Moreover, changes in the electronic state of the polyene moiety of Asx-*R* via intermolecular interaction with Cap were suggested to be crucial for the synergistic enhancement of

the antioxidative activity. These results suggest that antioxidative compounds that can induce changes in the electronic state of Asx via intermolecular interaction should work as enhancers of Asx function and that liposomes co-encapsulating Asx and such antioxidants may offer a hopeful antioxidant formulation for the prevention of oxidative stress in ROS-related diseases.

Acknowledgements

This research was supported by the Research Program for the Development of Intelligent Tokushima Artificial Exosome (iTEX) from Tokushima University.

Declaration of interest statement

The authors declare no competing financial interests.

References

[1] Harrison D, Griendling KK, Landmesser U, Hornig B, Drexler H. Role of oxidative stress in atherosclerosis. Am J Cardiol 2003;91(3):7-11.

[2] Shimokawa T, Yoshida M, Fukuta T, Tanaka T, Inagi T, Kogure K. Efficacy of high-affinity liposomal astaxanthin on up-regulation of age-related markers induced by oxidative stress in human corneal epithelial cells. J Clin Biochem Nutr 2018:18-27.

[3] Chan PH. Reactive oxygen radicals in signaling and damage in the ischemic brain. J Cereb Blood Flow Metab 2001;21(1):2-14.

[4] Group EAIS. Effect of a novel free radical scavenger, edaravone (MCI-186), on acute brain infarction. Randomized, placebo-controlled, double-blind study at multicenters. Cerebrovasc Dis 2003;15(3):222.

[5] Fukuzawa K. [10] Singlet oxygen scavenging in phospholipid membranes. Methods Enzymol.

Volume 319: Elsevier; 2000. p 101-110.

[6] Goto S, Kogure K, Abe K, Kimata Y, Kitahama K, Yamashita E, Terada H. Efficient radical trapping at the surface and inside the phospholipid membrane is responsible for highly potent antiperoxidative activity of the carotenoid astaxanthin. Biochim Biophys Acta Biomembr 2001;1512(2):251-258.

[7] Palozza P, Krinsky NI. Astaxanthin and canthaxanthin are potent antioxidants in a membrane model. Arch Biochem Biophys 1992;297(2):291-295.

[8] Hama S, Uenishi S, Yamada A, Ohgita T, Tsuchiya H, Yamashita E, Kogure K. Scavenging of hydroxyl radicals in aqueous solution by astaxanthin encapsulated in liposomes. Biol Pharm Bull 2012;35(12):2238-2242.

[9] Hama S, Takahashi K, Inai Y, Shiota K, Sakamoto R, Yamada A, Tsuchiya H, Kanamura K, Yamashita E, Kogure K. Protective effects of topical application of a poorly soluble antioxidant astaxanthin liposomal formulation on ultraviolet-induced skin damage. J Pharm Sci 2012;101(8):2909-16.

[10] Kamezaki C, Nakashima A, Yamada A, Uenishi S, Ishibashi H, Shibuya N, Hama S, Hosoi S, Yamashita E, Kogure K. Synergistic antioxidative effect of astaxanthin and tocotrienol by co-encapsulated in liposomes. J Clin Biochem Nutr 2016;59(2):100-106.

[11] Ishikawa M, Hirai S, Yoshida T, Shibuya N, Hama S, Takahashi Y, Fukuta T, Tanaka T, Hosoi S, Kogure K. Carotenoid Stereochemistry Affects Antioxidative Activity of Liposomes Co-encapsulating Astaxanthin and Tocotrienol. Chem Pharm Bull 2018;66(7):714-720.

[12] Kogure K, Goto S, Nishimura M, Yasumoto M, Abe K, Ohiwa C, Sassa H, Kusumi T, Terada H. Mechanism of potent antiperoxidative effect of capsaicin. Biochim Biophys Acta Gen Subj 2002;1573(1):84-92.

[13] Okada Y, Okajima H. Antioxidant effect of capsaicin on lipid peroxidation in homogeneous solution, micelle dispersions and liposomal membranes. Redox Rep 2001;6(2):117-122.

[14] Ray PS, Maulik G, Cordis GA, Bertelli AA, Bertelli A, Das DK. The red wine antioxidant

resveratrol protects isolated rat hearts from ischemia reperfusion injury. Free Radic Biol Med 1999;27(1-2):160-169.

[15] Stivala LA, Savio M, Carafoli F, Perucca P, Bianchi L, Maga G, Forti L, Pagnoni UM, Albini A, Prosperi E and others. Specific structural determinants are responsible for the antioxidant activity and the cell cycle effects of resveratrol. J Biol Chem 2001;276(25):22586-94.

[16] Price M, Reiners JJ, Santiago AM, Kessel D. Monitoring singlet oxygen and hydroxyl radical formation with fluorescent probes during photodynamic therapy. Photochem Photobiol 2009;85(5):1177-81.

[17] Jomova K, Valko M. Advances in metal-induced oxidative stress and human disease. Toxicology 2011;283(2-3):65-87.

[18] Grimme S, Ehrlich S, Goerigk L. Effect of the damping function in dispersion corrected density functional theory. J Comput Chem 2011;32(7):1456-65.

[19] Leela JS, Hemamalini R, Muthu S, Al-Saadi AA. Spectroscopic investigation (FTIR spectrum), NBO, HOMO-LUMO energies, NLO and thermodynamic properties of 8-Methyl-N-vanillyl-6-nonenamideby DFT methods. Spectrochim Acta A Mol Biomol Spectrosc 2015;146:177-86.

[20] Reed AE, Curtiss LA, Weinhold F. Intermolecular interactions from a natural bond orbital, donor-acceptor viewpoint. Chem Rev 1988;88(6):899-926.

[21] Jackson H, Braun CL, Ernst H. The chemistry of novel xanthophyll carotenoids. Am J Cardiol 2008;101(10A):50D-57D.

[22] Curek GD, Cort A, Yucel G, Demir N, Ozturk S, Elpek GO, Savas B, Aslan M. Effect of astaxanthin on hepatocellular injury following ischemia/reperfusion. Toxicology 2010;267(1-3):147-53.

[23] Lu YP, Liu SY, Sun H, Wu XM, Li JJ, Zhu L. Neuroprotective effect of astaxanthin on H(2)O(2)-induced neurotoxicity in vitro and on focal cerebral ischemia in vivo. Brain Res 2010;1360:40-8.

[24] Guerin M, Huntley ME, Olaizola M. Haematococcus astaxanthin: applications for human health and nutrition. Trends Biotechnol 2003;21(5):210-216.

[25] Pashkow FJ, Watumull DG, Campbell CL. Astaxanthin: a novel potential treatment for oxidative stress and inflammation in cardiovascular disease. Am J Cardiol 2008;101(10A):58D-68D.

Figure legends

Fig. 1. Chemical structures of astaxanthin (Asx); stereoisomers of Asx: 3R,3'R-form (Asx-R), 3S,3'S-form (Asx-S), and 3R,3'S-meso form (Asx-meso); capsaicin (Cap); and resveratrol (Res).

Fig. 2. Hydroxyl radical scavenging activity of liposomes encapsulating Cap (Cap-lipo) and Res (Res-lipo).

Relative antioxidative activities of Cap-lipo (A) and Res-lipo (B) were evaluated by the decrease in fluorescence intensity of APF which fluoresces via reaction with hydroxyl radicals. The decrease rate of the fluorescence intensity of APF in each liposomal group was calculated as the hydroxyl radical scavenging activity by setting the control group (plain EPC liposomes) as 100%. Data are the mean ± S.D. (n=3).

Fig. 3. Effect of liposomes co-encapsulating Asx and Res (Asx/Res-lipo) or Asx and Cap (Asx/Cap-lipo) on hydroxyl radical scavenging.

Relative hydroxyl radical scavenging activities of Asx/Res-lipo (A) and Asx/Cap-lipo (B) were evaluated using APF. White, gray, and black columns indicate the groups of Res- or Cap-lipo, Asx-lipo, and liposomes co-encapsulating two antioxidants, respectively. Additive values of the activity of each liposomal sample are denoted by dotted lines. (C) Results of the additive activity of Asx-lipo (1.88 μM) plus Cap-lipo (0.94 μM), which were respectively mixed in a test tube, and the synergistic antioxidative activity of Asx/Cap-lipo (Asx 1.88 μM/Cap 0.94 μM) are shown. With the control group (plain EPC liposomes) as 100%, the decreased percentage of the fluorescence intensity of APF in each group was calculated as the hydroxyl radical scavenging activity. Data are mean ± S.D. from three independent experiments. Significant difference; * $P<0.05$.

Fig. 4. Intermolecular interaction energies of Asx stereoisomers with Cap.

Intermolecular interaction energies of Asx stereoisomers with Cap were estimated using the Gaussian 09 program.

Fig. 5. Comparison of antioxidative activities of Asx-S and Asx-R co-encapsulated with Cap into liposomes.

Relative hydroxyl radical scavenging activities of Asx-*S*/Cap-lipo (A) and Asx-*R*/Cap-lipo (B) were evaluated using APF. White, gray, and black bars show Cap-lipo (0.94 μM), Asx-*S*- or Asx-*R*-lipo (0.47-7.5 μM), and Asx-*S*/Cap- or Asx-*R*/Cap-lipo, respectively. The combined values of the activity of each liposome sample are denoted by dotted lines. (C) The additive hydroxyl radical scavenging activity of Asx-*R*-lipo (0.47 μM) and Cap-lipo (0.94 μM), which were respectively mixed in a test tube, and the synergistic activity of Asx-*R*/Cap-lipo (Asx-*R* 0.47 μM/Cap 0.94 μM) are shown. The decrease rate of the APF fluorescence intensity in each liposome group was calculated as the hydroxyl radical scavenging activity by setting the control group (plain EPC liposomes) as 100%. Data are mean ± S.D. from the results of three independent experiments. Significant difference; * $P<0.05$.

Fig. 6. Influence of intermolecular interactions on bond dissociation energy (BDE) of the active sites of Asx-R and Cap.

The active sites of Asx-*R* (C3) and Cap (C7) are shown by dotted circles. The BDE of the active sites of Asx-*R* and Cap were calculated using the Gaussian 09 program as described in Material and Methods. The BDE of Asx-*R* alone and upon interaction with Cap, and that of Cap alone and upon interaction with Asx-*R* are indicated.

Fig. 7. Visible absorption spectra of liposomes co-encapsulating Asx-R and Cap.

The visible absorption spectra of Asx-*R*/Cap-lipo (black solid line) and that of a suspension

containing Asx-*R*-lipo and Cap-lipo (gray dotted line) were measured. The absorption spectrum of EPC liposomes without antioxidants was subtracted from the absorption spectrum of each antioxidant-encapsulated liposome to cancel liposomal turbidity. The peaks of the absorption spectra of Asx-*R*/Cap-lipo and a suspension containing Asx-*R*-lipo and Cap-lipo are indicated by black and white arrows, respectively.

Fig. 8. Influence of intermolecular interactions between Asx-R and Cap on electronic structures.

(A) Schematic showing intermolecular interactions of Asx-*R* half fragment A with Cap. (B) The electronic structure of Asx-*R* half fragment A upon interaction with Cap was compared with free Asx-*R* half fragment B. Electronic changes Δqi(complex-free) of Asx-*R* half fragment A complexed with Cap (closed circle, solid line) and free Asx-*R* half fragment B (open circle, dotted line) are shown. (C) Electronic change of Cap complexed with Asx-*R* is presented (open circle, solid line).

Fig. 1

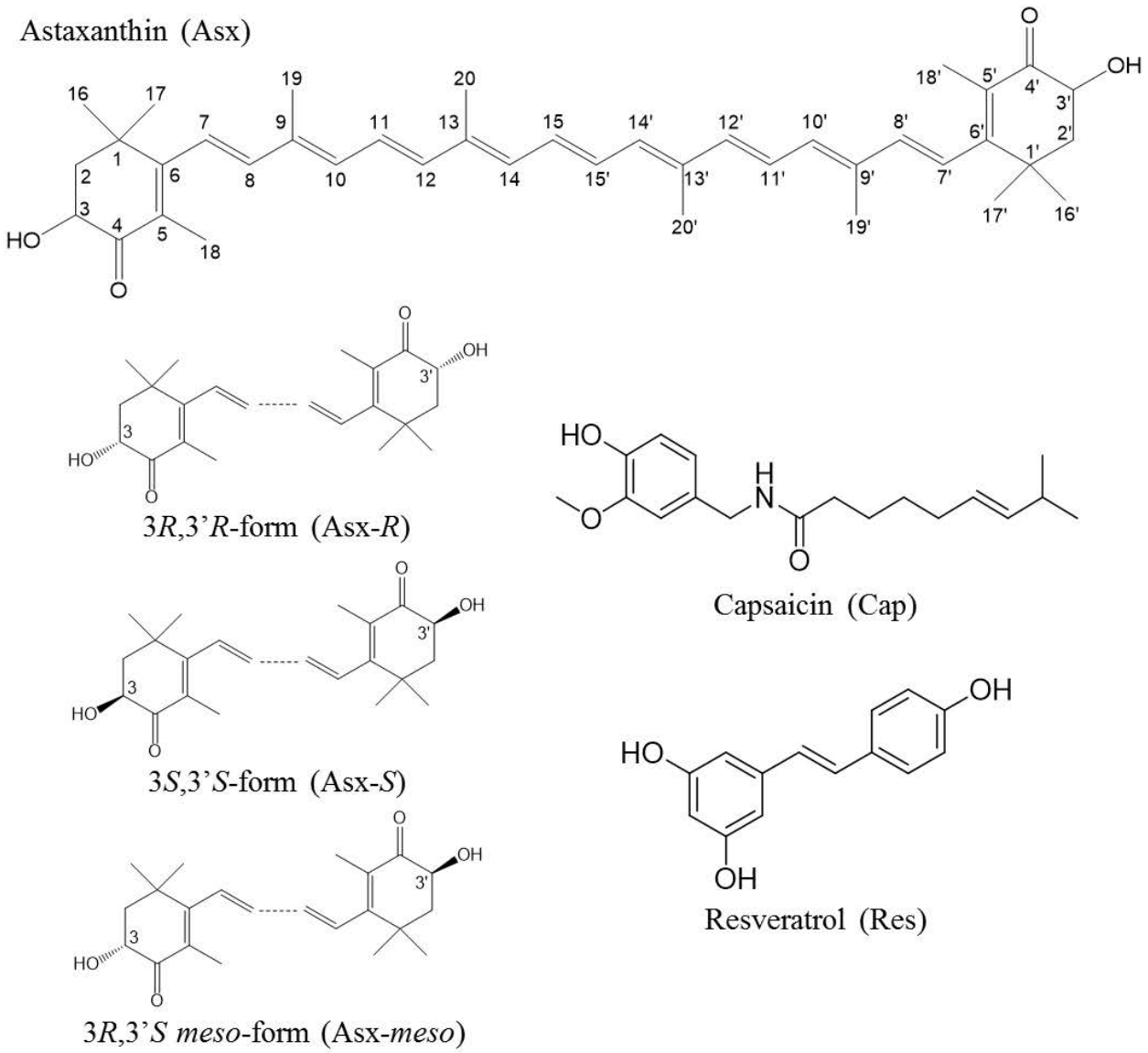
Astaxanthin (Asx)
3R,3'R-form (Asx-R)
Capsaicin (Cap)
3S,3'S-form (Asx-S)
Resveratrol (Res)
3R,3'S meso-form (Asx-meso)

Fig. 2

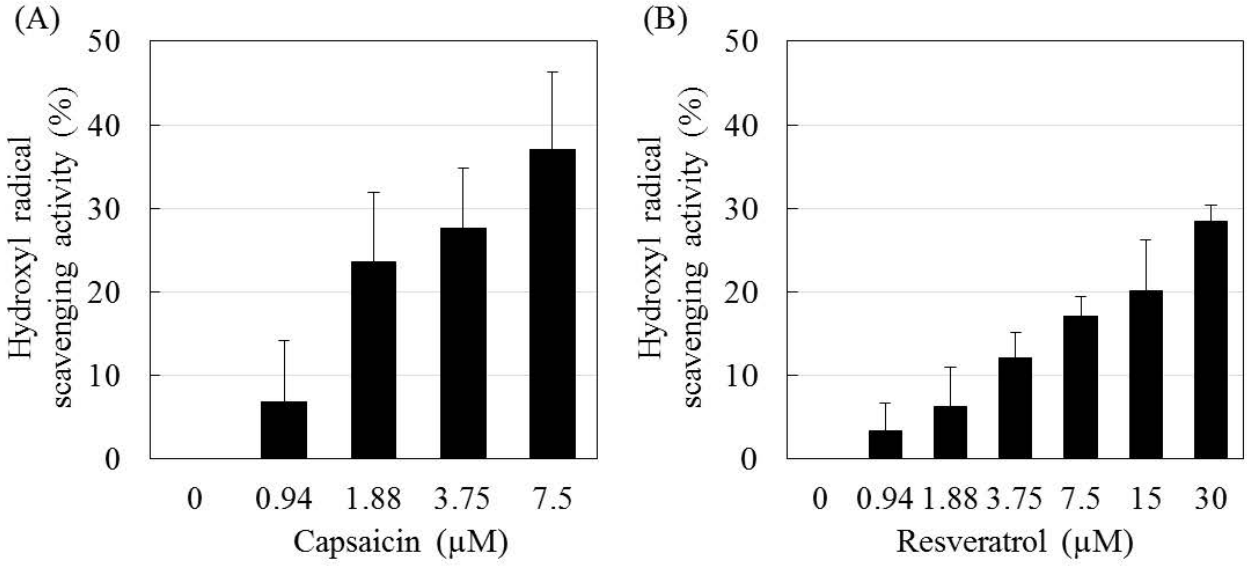
(A)
Hydroxyl radical scavenging activity (%)
50
40
30
20
10
0
0
0.94
1.88
3.75
7.5
Capsaicin (μM)
(B)
Hydroxyl radical scavenging activity (%)
50
40
30
20
10
0
0
0.94
1.88
3.75
7.5
15
30
Resveratrol (μM)

Fig. 3

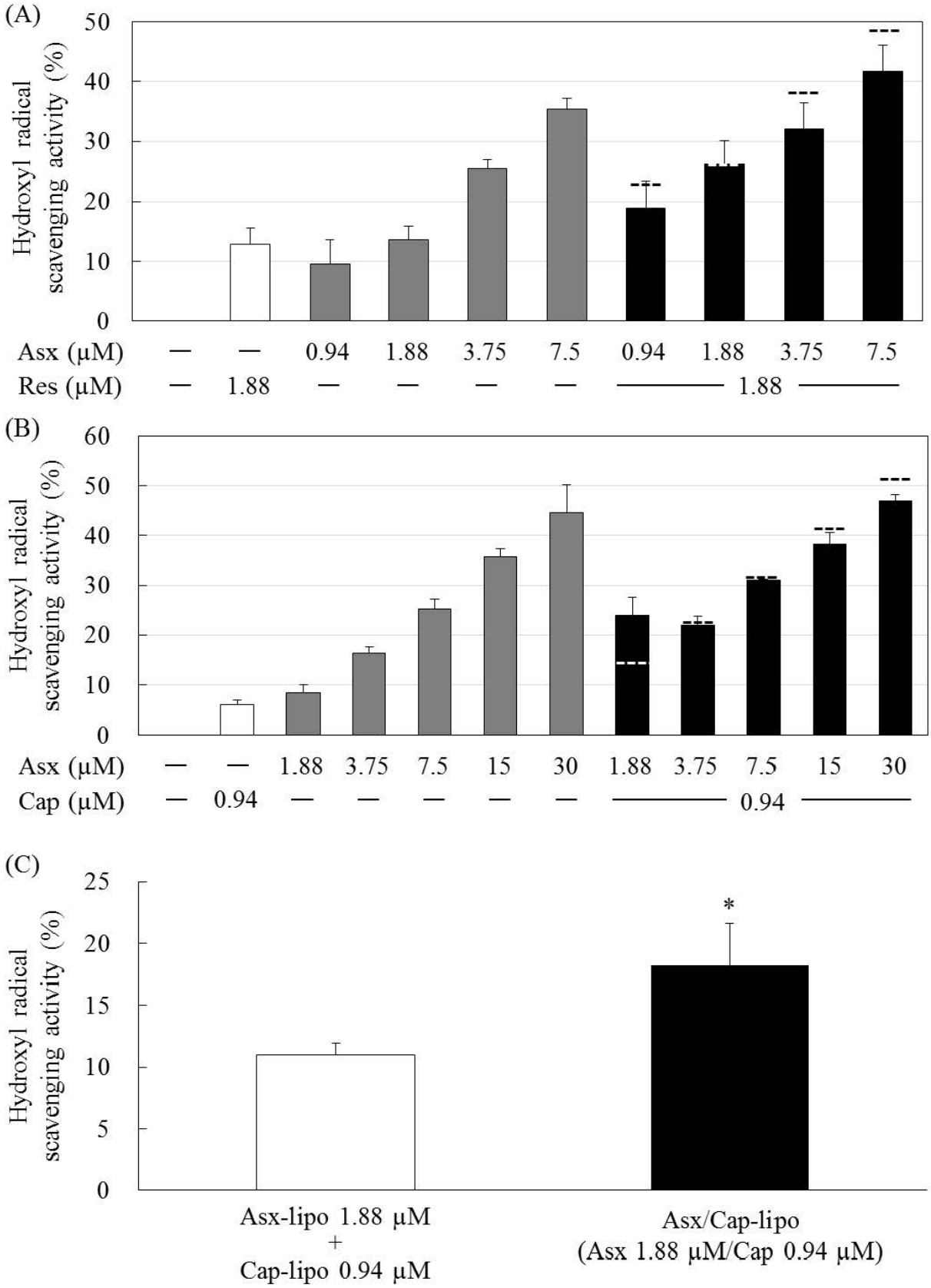
(A)
Hydroxyl radical scavenging activity (%)
50
40
30
20
10
0
Asx (μM) — — 0.94 1.88 3.75 7.5 0.94 1.88 3.75 7.5
Res (μM) — 1.88 — — — — 1.88
(B)
Hydroxyl radical scavenging activity (%)
60
50
40
30
20
10
0
Asx (μM) — — 1.88 3.75 7.5 15 30 1.88 3.75 7.5 15 30
Cap (μM) — 0.94 — — — — — 0.94
(C)
Hydroxyl radical scavenging activity (%)
25
20
15
10
5
0
*
Asx-lipo 1.88 μM
+
Cap-lipo 0.94 μM
Asx/Cap-lipo
(Asx 1.88 μM/Cap 0.94 μM)

Fig. 4

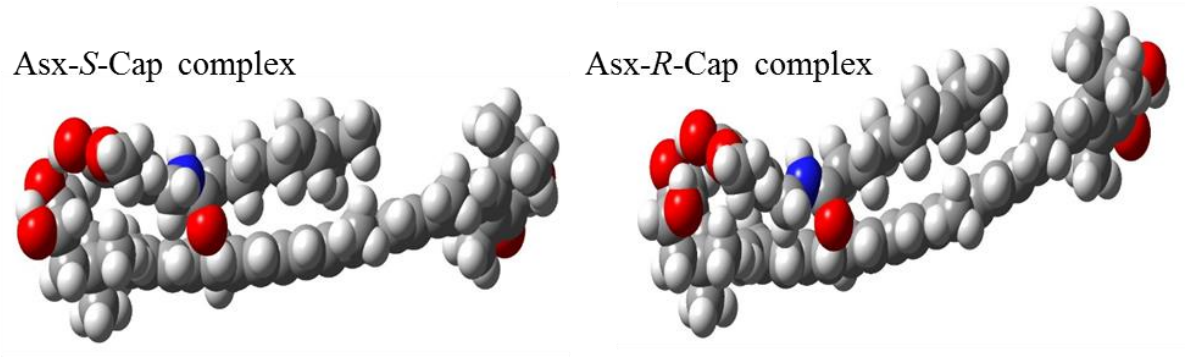

	Intermolecular interaction energy
Asx-*S*-Cap complex	26.05 kcal/mol
Asx-*R*-Cap complex	29.04 kcal/mol
Asx-*meso*-Cap complex	27.62 kcal/mol

Fig. 5

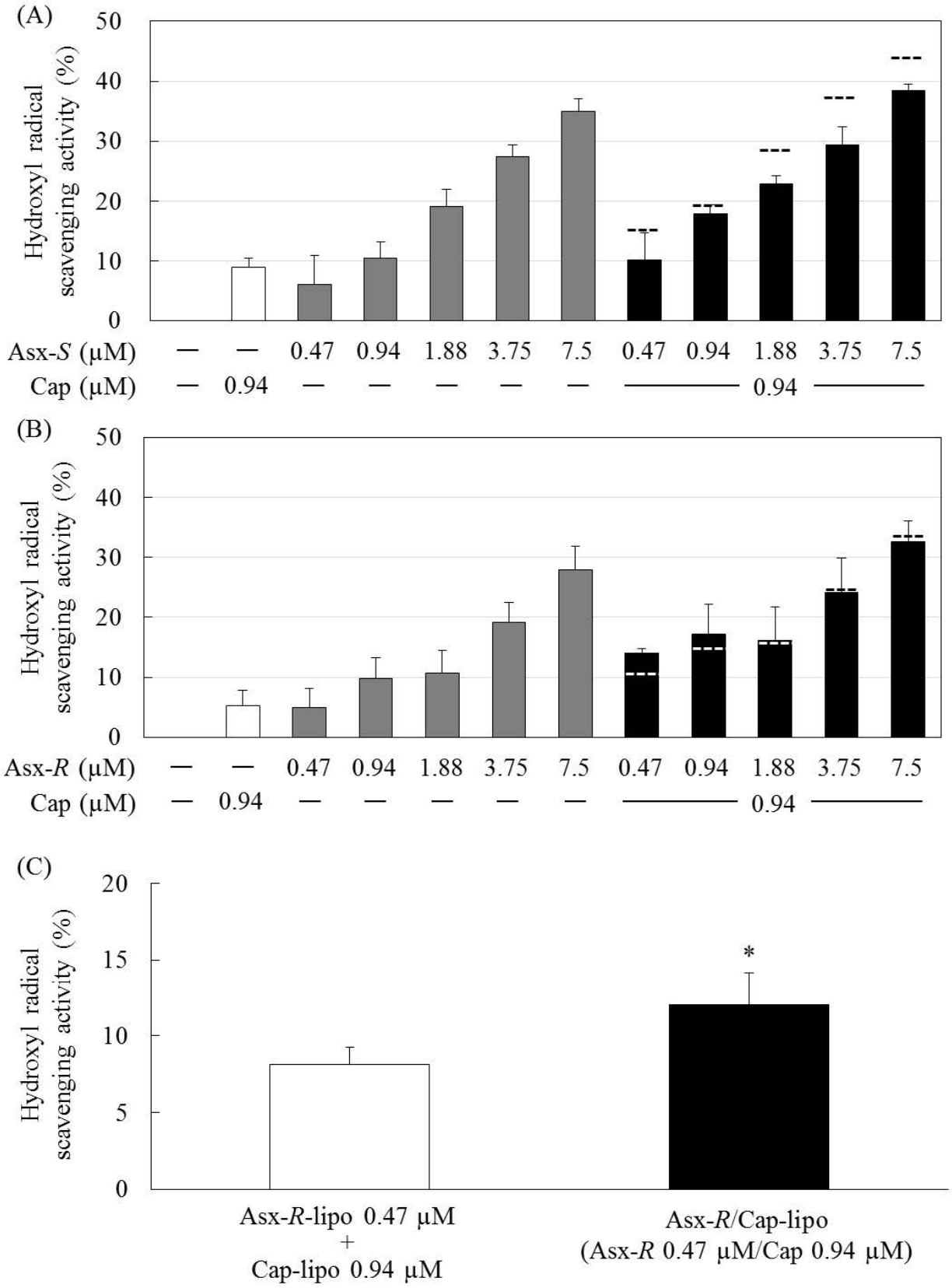
(A)
Hydroxyl radical scavenging activity (%)
50
40
30
20
10
0
Asx-S (μM) — — 0.47 0.94 1.88 3.75 7.5 0.47 0.94 1.88 3.75 7.5
Cap (μM) — 0.94 — — — — — 0.94
(B)
Hydroxyl radical scavenging activity (%)
50
40
30
20
10
0
Asx-R (μM) — — 0.47 0.94 1.88 3.75 7.5 0.47 0.94 1.88 3.75 7.5
Cap (μM) — 0.94 — — — — — 0.94
(C)
Hydroxyl radical scavenging activity (%)
20
15
10
5
0
*
Asx-R-lipo 0.47 μM
+
Cap-lipo 0.94 μM
Asx-R/Cap-lipo
(Asx-R 0.47 μM/Cap 0.94 μM)

Fig. 6

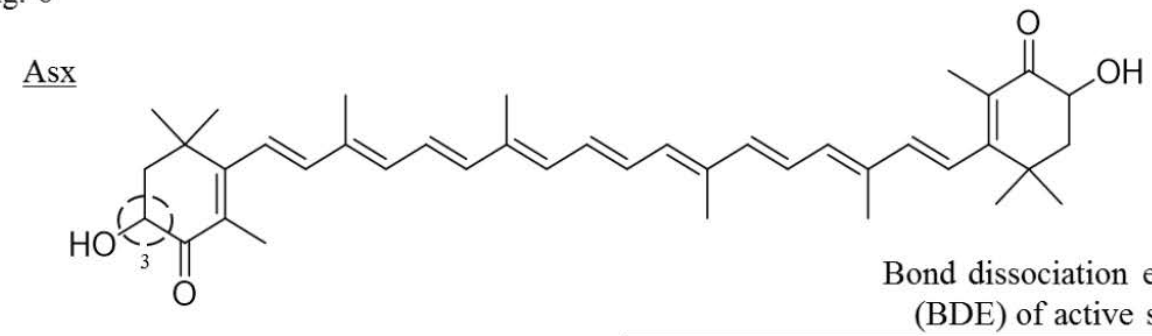

	Bond dissociation energy (BDE) of active sites
Asx-*R*	68.82 kcal/mol
Asx-*R*-Cap complex	68.56 kcal/mol
Cap	78.36 kcal/mol
Asx-*R*-Cap complex	78.33 kcal/mol

Fig. 7

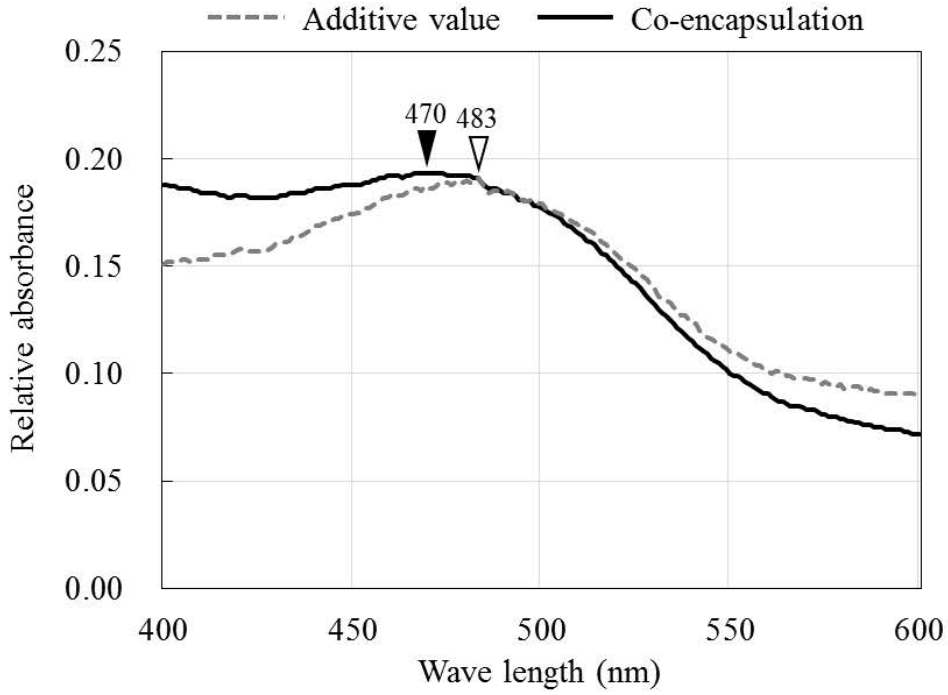

Fig. 7

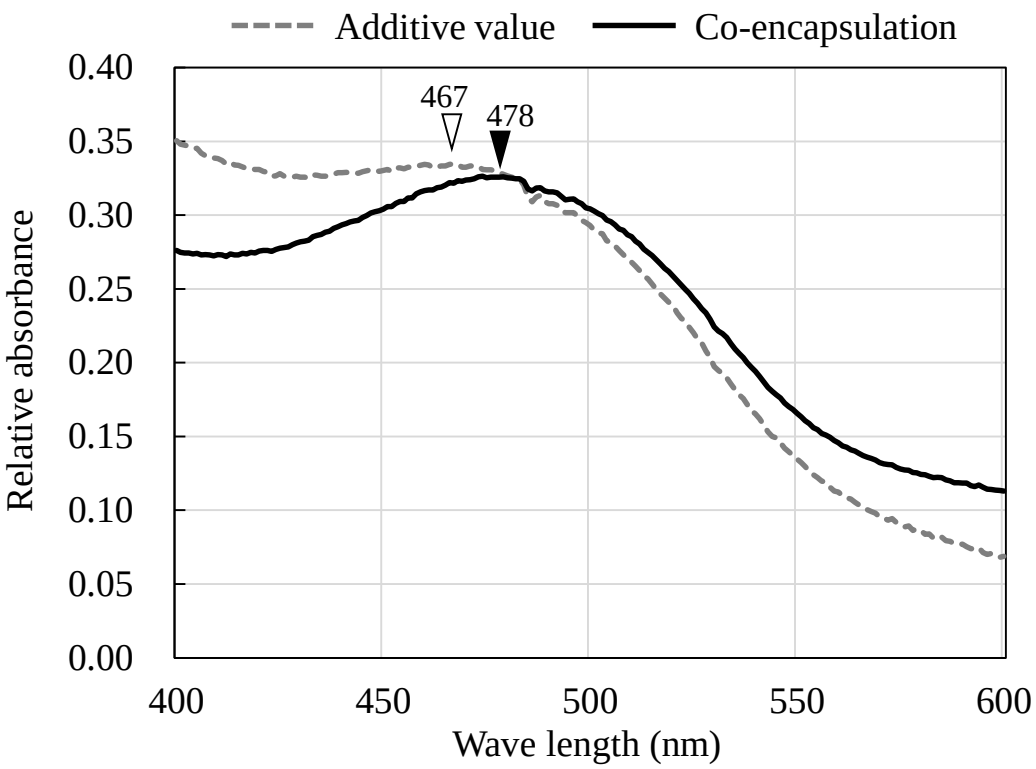
Additive value
Co-encapsulation
0.40
0.35
0.30
0.25
0.20
0.15
0.10
0.05
0.00
Relative absorbance
467
478
400
450
500
550
600
Wave length (nm)

Fig. 8

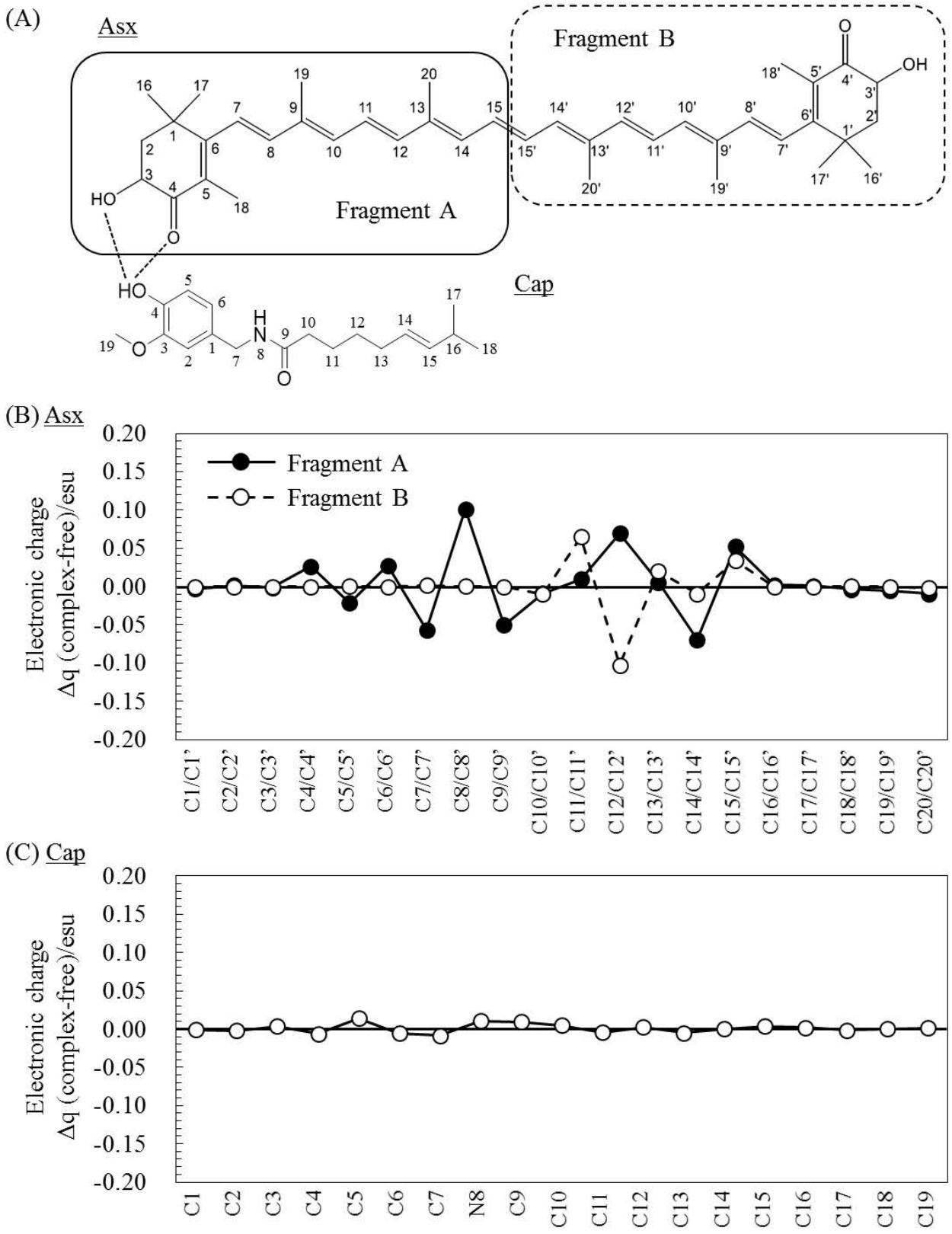
(A)
Asx
Fragment B
Fragment A
Cap
(B) Asx
Fragment A
Fragment B
Electronic charge
Δq (complex-free)/esu
0.20
0.15
0.10
0.05
0.00
-0.05
-0.10
-0.15
-0.20
C1/C1'
C2/C2'
C3/C3'
C4/C4'
C5/C5'
C6/C6'
C7/C7'
C8/C8'
C9/C9'
C10/C10'
C11/C11'
C12/C12'
C13/C13'
C14/C14'
C15/C15'
C16/C16'
C17/C17'
C18/C18'
C19/C19'
C20/C20'
(C) Cap
Electronic charge
Δq (complex-free)/esu
0.20
0.15
0.10
0.05
0.00
-0.05
-0.10
-0.15
-0.20
C1
C2
C3
C4
C5
C6
C7
N8
C9
C10
C11
C12
C13
C14
C15
C16
C17
C18
C19